NRC Research Press

ARTICLE

Investigation of metastability and instability effects on the minority carrier transport properties of microcrystalline silicon thin films by using the steady-state photocarrier grating technique[1]

Hamza Cansever, Mehmet Günes, Gökhan Yilmaz, H. Muzaffer Sagban, Vladimir Smirnov, Friedhelm Finger, and Rudolf Brüggemann

Abstract: Metastability effects in hydrogenated microcrystalline silicon thin films due to air, high purity nitrogen, helium, argon, and oxygen were investigated using temperature-dependent dark conductivity, photoconductivity, and steady-state photocarrier grating methods. It was found that short-term air, nitrogen, and inert gases caused a small reversible increase of σ_{Dark} and σ_{photo} within a factor of two, but they did not affect the minority carrier $\mu\tau$-products significantly. These changes are partially reduced by vacuum treatment and completely reduced after heat treatment at 430 K. However, oxygen gas treatment at 80 °C resulted in more than an order of magnitude increase in both σ_{Dark} and σ_{photo} and an increase in the diffusion length, $L_{D,}$ by 50% from that of the annealed-state value in highly crystalline samples, while no significant metastability is detected in amorphous and low crystalline silicon thin films. A following heat treatment partially recovers both σ_{Dark} and σ_{photo} to their annealed-state values, while L_D decreases only slightly. Such increase in the L_D values could be due to a decrease in the density of recombination centers for holes below the Fermi level, which may be related to passivation of defects by oxygen on the surface of crystalline grains.

PACS Nos.: 73.61.Jc, 73.63.Bd, 73.50.Pz, 72.80.Ng.

Résumé : Nous étudions les effets de la métastabilité dans des films minces de silicium microcristallins hydrogénés dû à de l'air, de l'azote très pur, de l'hélium, de l'argon et de l'oxygène, en utilisant la dépendance en température de la conductivité en obscurité, la photoconductivité et la méthode de *photocarrier grating* en régime stationnaire. Nous trouvons qu'à court terme, l'air, l'azote et les gaz inertes causent de petites augmentations réversibles de σ_{Dark} et σ_{photo} à l'intérieur d'un facteur deux, mais n'affectent pas de façon significative les porteurs minoritaires $\mu\tau$. Ces changements sont partiellement réduits par un traitement par le vide et le sont complètement après chauffage à 430 K. Cependant, le traitement à l'oxygène à 80 °C cause une augmentation de plus d'un ordre de grandeur de σ_{Dark} et σ_{photo} et une augmentation de 50 % de la longueur de diffusion L_D, comparé à la valeur d 'échantillons cristallins recuits, alors qu'aucune métastabilité n'est détectée dans les films minces de silicium amorphe et faiblement cristallin. Un chauffage subséquent ramène partiellement σ_{Dark} et σ_{photo} à leur valeur de recuit, mais L_D ne diminue qu'un peu. Une telle augmentation de L_D pourrait être due à une diminution de la densité des centres de recombinaison sous le niveau de Fermi et peut être reliée à la passivation des défauts par l'oxygène sur les grains cristallins de la surface. [Traduit par la Rédaction]

1. Introduction

Hydrogenated microcrystalline silicon (μc-Si:H) has been extensively studied for the last two decades and successfully applied as an absorber layer in thin film silicon solar cells [1, 2]. Materials with significant crystallinity, and solar cells with such an absorber layer, were found to be almost immune to the Staebler–Wronski effect [3] discovered in hydrogenated amorphous silicon (a-Si:H) thin films. However, optoelectronic properties of μc-Si:H films showed metastable changes after intentional or unintentional exposure to different atmospheric conditions [4, 5]. The first detailed study of Veprek et al. indicated that dark conductivity, σ_{Dark}, of highly conductive μc-Si:H films decreased by several orders of magnitude after samples were exposed to air and (or) to pure oxygen gas, indicating both reversible and irreversible changes [4]. Almost two decades later, it was demonstrated by Finger et al. that both decrease and increase in σ_{Dark} occurred as high quality μc-Si:H samples were exposed to atmospheric ambient, as well as to oxygen gas [5]. Since then most of the investigations carried out on the metastability effects have used techniques that mainly focus on the characterization of the majority carrier transport properties [5–7]. It is important to note that such metastable changes may eventually affect the operation of thin film silicon solar cells, as the collection of charge carriers is determined by both majority and minority carrier transport properties of the absorber layer [8]. Even though similar transport models have been proposed for the majority and minority carriers of a-Si:H and μc-Si:H films deposited by very high frequency – plasma enhanced chemical vapor deposition (VHF-PECVD) techniques, the metastability effects due to atmospheric exposures on the minority carrier transport properties were not clearly demonstrated in those

Received 24 October 2013. Accepted 17 January 2014.

H. Cansever, M. Günes, G. Yilmaz, and H.M. Sagban. Department of Physics, Faculty of Sciences, Mugla Sitki Kocman University, Kotekli Yerleşkesi, Mugla, Turkey.
V. Smirnov and F. Finger. Forschungszentrum Jülich, IEK-5 Photovoltaik, 52425 Jülich, Germany.
R. Brüggemann. Institut für Physik, Carl von Ossietzky Universität Oldenburg, 26111 Oldenburg, Germany.
Corresponding author: Mehmet Günes (e-mail: mehmet.gunes@mu.edu.tr).

[1]This paper was presented at the 25th International Conference on Amorphous and Nanocrystalline Semiconductors (ICANS25).

reports [9–12]. Most recent investigation by Brüggemann et al. indicated that no significant metastable changes in the minority carrier transport properties were caused by the atmospheric exposures even though large changes occurred in the σ_{Dark} and σ_{photo} [13], which were attributed to the band bending at the surface due to charging of defects. In this study, careful attention has been paid to obtain the steady-state condition of dark conductivity of samples before measuring the metastable changes in minority carrier diffusion lengths by using steady-state photocarrier grating (SSPG) technique [14], and these results were correlated with those obtained from temperature-dependent dark conductivity and steady-state photoconductivity methods.

2. Experimental details

Hydrogenated microcrystalline silicon thin films were deposited on smooth glass substrates using the VHF-PECVD technique under different silane gas ratios (SC = $SiH_4/(SiH_4 + H_2)$) and at a substrate temperature of 190 °C. Thickness of the samples was ~300 nm. Their crystalline volume fraction, ($I_C^{RS} = (I_{500} + I_{520})/(I_{480} + I_{520} + I_{500})$), was obtained from Raman measurements changes from 0 to 0.79. Silver coplanar electrodes were evaporated on the samples with 0.5 cm length and 0.5 mm separation. The samples were exposed to (*i*) ambient atmosphere at room temperature in the dark to cause uncontrolled metastability effect as well as (*ii*) a controlled gas ambient such as high purity nitrogen, helium, argon, and oxygen in a vacuum cryostat. Inert gas and nitrogen exposures were performed at 300 K, and oxygen gas treatment was carried out at 353 K. To record the metastable changes created in the sample, a computer-controlled time-dependent dark conductivity measurement procedure has been developed and used in this study as defined in ref. 15. Measurements to probe the changes after treatments were performed at 300 K in the steady-state condition of dark conductivity in both exposing gas ambient as well as in high vacuum of 2–3 × 10^{-6} mbar. Temperature-dependent dark conductivity, intensity-dependent steady-state photoconductivity (SSPC), and steady-state photocarrier grating (SSPG) methods have been used to detect the changes in the metastable state and after annealing. SSPC measurements were done using He–Ne laser with photon flux ranging from 1 × 10^{13} to 4 × 10^{17} $cm^{-2}s^{-1}$. SSPG measurements were performed for flux values between 4 × 10^{16} and 2 × 10^{17} $cm^{-2}s^{-1}$ with an applied DC bias in the ohmic and low field region, where only diffusion controlled transport dominates. Minority carrier hole diffusion lengths, L_D, were determined from the SSPG measurements by using both nonlinear [14] and linear [16] fits of experimentally obtained β (= J_{coh}/J_{incoh}) versus Λ results in (1) and (2), respectively,

$$\beta = 1 - \frac{2\phi}{\left[1 + \left(4\pi^2 L_D^2/\Lambda^2\right)\right]^2} \quad (1)$$

$$\frac{1}{\Lambda^2} = \frac{\sqrt{\phi}}{\left(4\pi^2 L_D^2\right)}\sqrt{\frac{2}{1-\beta}} - \left(4\pi^2 L_D^2\right)^{-1} \quad (2)$$

where ϕ fit parameter was defined as the grating quality parameter [14]. Metastable changes in the majority and minority carrier mobility-lifetime $(\mu\tau)_{n,p}$-products were obtained from the experimental SSPC and SSPG measurements.

3. Results and discussion

3.1. The effects of inert gas and nitrogen exposures

Hydrogenated microcrystalline silicon thin films with high crystalline volume fraction may represent both increase and decrease in room temperature dark conductivity [5] as samples are exposed to open air or different gas ambient as well as subjected to different heat or vacuum treatments. In addition, the changes in σ_{Dark} are also affected by the measurement ambient resulting in large difference in air and in vacuum [13]. As a result, σ_{Dark} will strongly depend on the sample history. It then becomes more difficult to compare the results even on the same sample or with results published in the literature for similar quality films characterized using the same measurements [13, 16]. In Fig. 1, changes in σ_{Dark} are presented for annealed μc-Si:H samples with $I_C^{RS} = 0.68$, as exposed to different ambients for up to 60 h. SSPC and SSPG measurements were performed in gas ambient and in vacuum when σ_{Dark} was almost stable with time. The dark conductivity values, which are considered as "stabilized" and where further SSPC and SSPG experiments were performed, are indicated by vertical arrows in Fig. 1. A summary of room temperature σ_{Dark} and σ_{photo} is presented in Fig. 2*a* for different gas exposures and following annealing processes as explained above. It was found that short-term air exposure, inert gasses, and nitrogen cause an

Fig. 1. Time-dependent dark conductivity for a microcrystalline silicon sample with $I_C^{RS} = 0.68$ when exposed to inert gas and nitrogen ambients (symbols) and in the following vacuum process (dashed, dotted, and dashed–dotted lines) carried out after each exposure. Air-exposed state was first measured in air, then in vacuum (black stars). SSPC and SSPG measurements were performed as dark conductivity remained almost unchanged with time as indicated by vertical arrows.

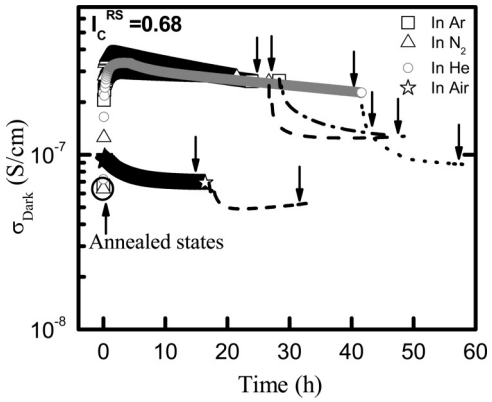

Fig. 2. The effect of metastable changes on the (*a*) room temperature σ_{Dark} and σ_{photo}, and (*b*) minority carrier diffusion lengths, L_D, after short-term air, inert gas, and nitrogen exposures and following annealing processes for a μc-Si:H sample with $I_C^{RS} = 0.68$.

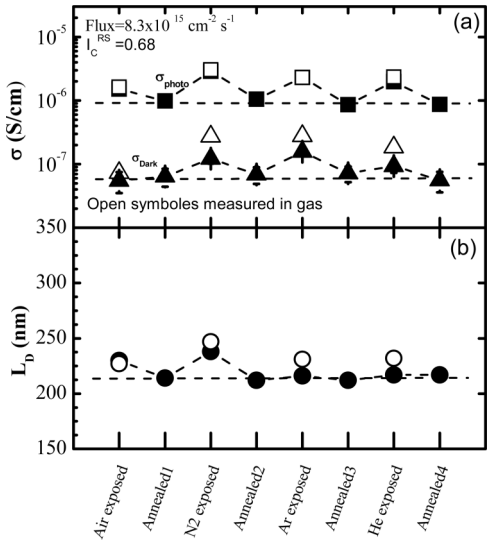

Fig. 3. Experimental β versus grating period Λ for the annealed states carried out after each inert gas and nitrogen treatment and for argon-exposed state measured in vacuum for a μc-Si:H sample with I_C^{RS} = 0.68.

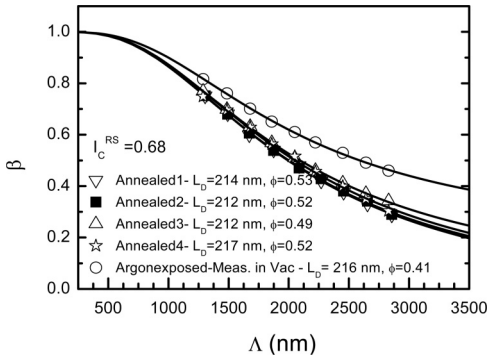

increase in σ_{Dark} and σ_{photo} in the metastable state. Such metastable increases in σ_{Dark} and σ_{photo} were found to be reversible after an annealing process performed at 430 K. σ_{Dark} values measured in exposing gas ambient are higher within a factor of two to three than those measured in vacuum, while σ_{photo} values are almost unaffected. The effect of metastable changes on minority carrier diffusion lengths obtained from SSPG measurements is shown in Fig. 2*b* for the above defined conditions. There is a slight increase in L_D after short-term air, inert gas, and nitrogen exposures within 5–10 nm, which is completely reversible by either vacuum or annealing. This is presented in Fig. 3 that experimental β versus Λ curves are almost identical for the annealed states measured before and after inert gas and nitrogen treatments. Nonlinear fits to the experimental data resulted in L_D values of 214 ± 3 nm in the annealed states. Experimentally obtained σ_{photo} and L_D values were used to calculate majority and minority carrier $\mu\tau$-products for the annealed, inert gas, and nitrogen-exposed states. These results are presented in Fig. 4 as a function of dark conductivity, corresponding to the dark conductivity values shown in Fig. 2. It is seen that majority carrier $\mu\tau$-products tend to increase with the increase in σ_{Dark}. However, minority carrier $\mu\tau$-products are slightly affected as previously reported by Brüggemann et al. [13].

We realize that the observed changes in the transport properties of the μc-Si:H materials upon storage or treatment of the samples in inert gas or nitrogen are unexpected. Ar, He, and N_2 molecule are electro-neutral and should not cause an induced surface charge as they are in contact with the sample surface. In an earlier report, where nitrogen exposure caused a reversible dark conductivity decrease in highly crystalline and highly conductive microcrystalline silicon films [17], the effect was attributed to the residual atmospheric gas impurities in the nitrogen tank. We would not expect a similar source of contamination in our study, where 5N grade high purity gases were used and gas supply lines and the cryostat vacuum system was pumped and purged several times before gas exposure and measurement. However, a remaining gas impurity cannot be 100% excluded. This or possible other mediated effects by the storage and measurement in Ar, He, and N_2, such as small changes in sample temperature, need to be further examined. We note that the effect is completely reversible after annealing as generally observed for the metastable changes after short-term air exposure [4–7]. Furthermore, minority carrier diffusion lengths and $\mu\tau$-products for holes are almost unaffected as previously reported for reversible conductivity changes [13].

3.2. The effects of oxygen exposures

Time-dependent σ_{Dark} of a highly crystalline intrinsic sample with I_C^{RS} = 0.79 is presented in Fig. 5. Oxygen exposure at 353 K

Fig. 4. Mobility-lifetime product for majority and minority carriers obtained from steady-state photoconductivity and steady-state photocarrier grating method as a function of dark conductivity changes due to inert gas and nitrogen exposures and following annealing processes for a μc-Si:H sample with I_C^{RS} = 0.68.

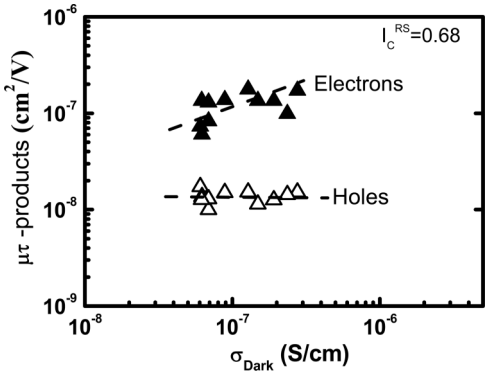

Fig. 5. Time-dependent dark conductivity for a high crystalline microcrystalline silicon sample with I_C^{RS} = 0.79 when exposed to oxygen at 353 K, cooled to 300 K in O_2, and following vacuum process at 300 K. SSPC and SSPG measurements were performed when σ_{Dark} remained unchanged with time as indicated by vertical arrows.

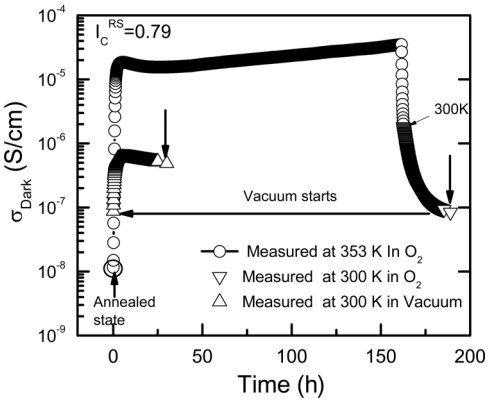

caused an increase in σ_{Dark} more than three orders of magnitude due to temperature and oxygen exposure. At the end of 160 h of exposure, the sample was cooled to 300 K in oxygen ambient. Room temperature σ_{Dark} decreased slowly until a constant steady-state value, which was almost one order of magnitude higher than that of the annealed state. After SSPC and SSPG measurements were performed in oxygen ambient; the following vacuum process caused further increase in σ_{Dark} and reached a steady-state value as seen in Fig. 5 [13]. Room temperature σ_{Dark} increased by a factor of 50 in the oxygen-exposed state and following annealing process (Annealed2 in the figures) partially removed the metastability.

Steady-state photoconductivity measurements carried out at the steady-state condition of σ_{Dark} are presented in Fig. 6 for the oxygen-exposed state and the annealed states performed before and after the treatment. σ_{photo} versus flux increased by a factor of two as measured in oxygen ambient (shown by up and down triangles, respectively) without any change in the exponent γ, slope of σ_{photo} versus flux in a Log–Log plot. However, a more significant increase in σ_{photo} occurred (shown by open circles) as the sample was measured in high vacuum. Further increase in $\sigma_{photo,}$ as well as a decrease in the exponent γ from 0.74 to 0.60, was caused by the vacuum treatment as presented in Fig. 6. Such a metastable increase in σ_{photo} was partially minimized by the following annealing process, indicating that a presence of a par-

Fig. 6. Steady-state photoconductivity versus incoming flux in the oxygen-exposed state measured in oxygen and following vacuum as well as in the annealed states before and after oxygen exposure for a high crystalline microcrystalline silicon sample with $I_C^{RS} = 0.79$.

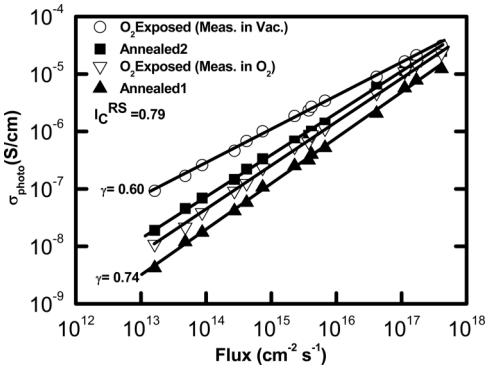

tial irreversible effect exists after oxygen treatment. Such an increase in σ_{Dark} and σ_{photo} may be attributed to the adsorption and bonding of oxygen on the surface of crystalline grains, causing a shift of the Fermi level due to the changes in the surface charge or changes in the density of defect distributions [6]. The changes in the occupation of defect states in the bandgap through the recombination process affect the majority and minority carrier $\mu\tau$-products.

In Fig. 7, the results of SSPG measurements are presented in a form of so-called Balberg plot [18] for the air- and oxygen-exposed states as well as for the annealed states carried out before and after exposures. Ambipolar diffusion length, L_D, measured in O_2 ambient after exposure increases from the annealed-state value of 175 nm to 200 nm. Further increase in L_D was observed as the sample was measured in high vacuum conditions, similar to dark and photoconductivity results presented above. L_D measured in vacuum for the oxygen-exposed state is almost 50% higher than that of annealed1 state measured before oxygen exposure. Such improvement in minority carrier diffusion lengths in oxygen-exposed state indicates that the density of recombination centers for the minority carriers (holes) should decrease and $\mu\tau$-products for holes should increase due to exposure to oxygen ambient. In Fig. 8, $\mu\tau$-products for majority and minority carriers are presented (filled symbols) as a function of room temperature dark conductivity obtained in the exposed states as well as annealed states for samples with $I_C^{RS} = 0.79$. As σ_{Dark} increases, majority carrier $\mu\tau$-products show similar increase as in inert gas and nitrogen-treated states presented in Fig. 4 [13]. However, $\mu\tau$-products for holes also increase with dark conductivity in contrast to that observed for inert gas treated states (see Fig. 4). In addition, the effect of oxygen on the $\mu\tau$-products for samples with $I_C^{RS} = 0.68$ is also shown in Fig. 8 (open symbols). In this compact sample, $\mu\tau$-products for holes increased irreversibly after oxygen exposure even though changes in σ_{Dark} and σ_{photo} were reversible.

The above results have shown that significant metastability and instability effects can be created in microcrystalline silicon thin films with $I_C^{RS} \geq 0.68$ by an exposure to oxygen gas. Similar experiments were also carried out on amorphous and low crystalline compact silicon films ($I_C^{RS} = 0.27$). A summary of the metastability effect on conductivities and minority carrier diffusion length, L_D, is presented in Fig. 9 as a function of crystalline volume fraction I_C^{RS}. Very little changes were observed in amorphous and low crystalline compact silicon films, consistent with electron spin resonance (ESR) study carried out on similar quality films under similar oxygen treatment conditions [19]. Furthermore, the reversible and irreversible effects in ESR spin density due to oxygen exposure were found to be larger in highly crystalline silicon films classified as type I with $I_C^{RS} > 0.79$ [19]. This class of materials has

Fig. 7. Linear plots (Balberg plots [18]) for $(2/(1-\beta))^{1/2}$ versus $1/\Lambda^2$ obtained from SSPG measurements for the oxygen-exposed state and annealed states carried out before and after exposure for a high crystalline microcrystalline silicon sample with $I_C^{RS} = 0.79$.

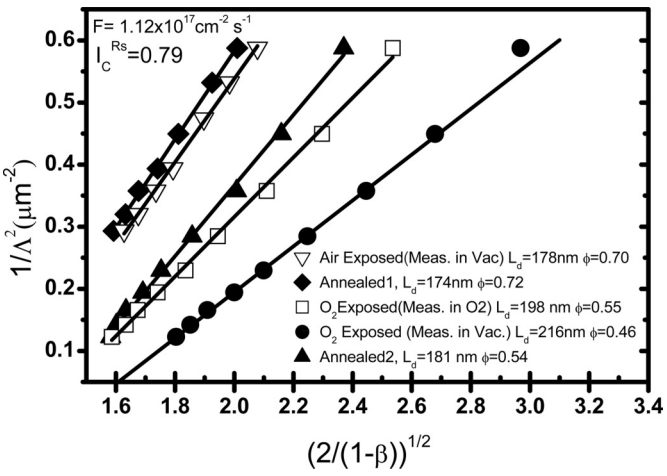

Fig. 8. Mobility-lifetime products for majority and minority carriers obtained from SSPC and SSPG methods as a function of dark conductivity changes due to oxygen exposure and annealed states carried out before and after exposure for μc-Si:H samples with $I_C^{RS} = 0.79$ (filled symbols) and $I_C^{RS} = 0.68$ (open symbols). Lines are guide to eye.

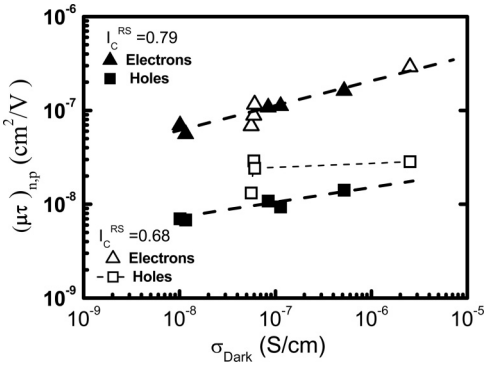

Fig. 9. Summary of the changes after oxygen treatment for (*a*) conductivities, the open symbols are for σ_{photo} and the filled symbols are for σ_{Dark}, and (*b*) minority carrier diffusion lengths as a function of crystalline volume fraction. The same symbols in (*b*) indicate the same states in (*a*).

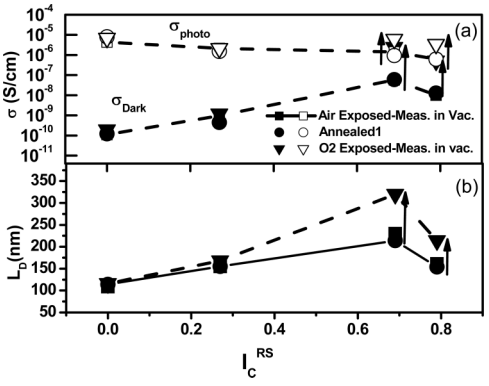

porous microstructure and allows in-diffusion of oxygen and other atmospheric gasses easily. It was reported that such a class of microcrystalline silicon films were highly conductive in the annealed state with activation energy between 0.1 and 0.25 eV [4, 5, 16]. Their dark conductivity decrease more than an order of magnitude after air and (or) oxygen exposure, resulting in an increase in activation energy and an increase in ESR spin density [4, 5, 19]. The sample with higher crystalline volume fraction (I_C^{RS} = 0.79) studied in this work can be considered as type I and porous in nature. In contrast to previous reports, the conductivity type is closer to an intrinsic case with an activation energy of 0.45 eV before oxygen exposure and decreased to 0.33 eV after oxygen treatment, resulting in an irreversible increase in σ_{Dark} and σ_{photo} in addition to the reversible changes removed by the annealing at 430 K. It was also found that minority carrier diffusion length, L_D, and minority carrier (hole) $\mu\tau$-products showed significant increase after oxygen treatment as shown in Fig. 8, which was also partially irreversible. The irreversible changes in minority carrier transport properties after oxygen exposure were not reported before, even though reversible changes due to short-term air exposure and (or) inert gas treatment shown in Fig. 4 are consistent with previous investigation [13]. The metastable changes in σ_{Dark} and σ_{photo} of compact samples with I_C^{RS} = 0.68 after oxygen treatment are almost reversible without any change in the activation energy of 0.48 eV. However, it was found that a further irreversible increase in minority carrier diffusion length and hole $\mu\tau$-products existed after the oxygen treatment as presented in Fig. 8 (open symbols).This indicates a decrease in the density of recombination centers for holes below the Fermi level, similar to what was found for highly crystalline samples. This could be caused by the in-diffusion of oxygen through cracks and chemical bonding on the surface of grain boundaries as suggested before [4–6, 16, 19]. This observation was independently confirmed by the sub-bandgap absorption measurements that oxygen and water exposure caused a significant decrease in the absorption coefficient spectrum at sub-bandgap energy region due to a decrease in the density of occupied defect states below the Fermi level [20]. Therefore, the methods using the majority carrier transport properties alone are not sufficient to understand the complex nature of metastability effect in heterogeneous microcrystalline silicon films as pointed out previously [13]. SSPG method provides additional information about the changes in the minority carriers transport properties as reported here.

4. Summary and conclusion

The effects of gas exposure on the transport properties of μc-Si:H films were investigated. A small reversible metastable increase in σ_{Dark} and σ_{photo}, as well as in the minority carrier diffusion length, L_D, was found upon short-term air, inert gas, and nitrogen exposure of microcrystalline samples. This effect can be minimized by a vacuum treatment and completely removed by the following heat treatment. Majority carrier $\mu\tau$-products increase with increasing dark conductivity. However, minority carrier $\mu\tau$-products are almost insensitive to the dark conductivity changes consistent with previous reports. Exposure of the materials to oxygen results in large reversible and irreversible changes of the transport properties in highly crystalline silicon films. This effect is more pronounced as measurements are carried out in vacuum after the treatment of the sample in oxygen atmosphere at 353 K. More than one order of magnitude increase in σ_{Dark} and σ_{photo} was observed, which was completely reversible for compact samples and partially irreversible for the highly crystalline porous material. In addition, an irreversible increase in the minority carrier diffusion lengths and $\mu\tau$-products were observed after oxygen treatment in both highly crystalline and compact materials. This could be due to an apparent decrease in the density of recombination centers for holes below Fermi level in the oxygen-exposed state, which in turn, may be related to passivation of defects on the surface of grains by oxygen. Further investigation is necessary to understand the nature and energy distribution of these defects in the bandgap and changes created due to exposure of the material to oxygen or water.

Acknowledgements

This work is financially supported by TÜBİTAK of Turkey (project No. 108T218) and the BMBF of Germany (project No. TUR 08/003).

References

1. J. Meier, R. Flückiger, H. Keppner, and A. Shah. Appl. Phys. Lett. **65**, 860 (1994). doi:10.1063/1.112183.
2. O. Vetterl, R. Carius, L. Houben, C. Sholten, L. Luysberg, A. Lambertz, F. Finger, and H. Wagner. Mat. Res. Soc. Symp. Proc. **609**, A15.2 (2000).
3. D.L. Staebler and C.R. Wronski. Appl. Phys. Lett. **31**(4), 292 (1977). doi:10.1063/1.89674.
4. S. Veprek, Z. Iqbal, R.O. Kühnhe, P. Capezzuto, F.-A. Sarrot, and J.K. Gimzewski. J. Phys. C Solid State Phys. **16**, 6241 (1983). doi:10.1088/0022-3719/16/32/015.
5. F. Finger, R. Carius, T. Dylla, S. Klein, S. Okur, and M. Gunes. IEE Circuits Devices Syst. **150**, 300 (2003). doi:10.1049/ip-cds:20030636.
6. V. Smirnov, S. Reynolds, C. Main, F. Finger, and R. Carius. J. Non-Cryst. Solids, **338–340**, 421 (2004). doi:10.1016/j.jnoncrysol.2004.03.010.
7. V. Smirnov, S. Reynolds, F. Finger, R. Carius, and C. Main. J. Non-Cryst. Solids, **352**, 1075 (2006). doi:10.1016/j.jnoncrysol.2005.12.014.
8. M. Sendova-Vassileva, S. Klein, and F. Finger. Thin Solid Films, **501**, 252 (2006). doi:10.1016/j.tsf.2005.07.148.
9. M. Goerlitzer, N. Beck, P. Torres, J. Meier, N. Wyrsch, and A. Shah. J. Appl. Phys. **80**, 5111 (1996). doi:10.1063/1.363491.
10. C. Droz, M. Goerlitzer, N. Wyrsch, and A. Shah. J. Non-Cryst. Solids, **266–269**, 319 (2000). doi:10.1016/S0022-3093(99)00718-8.
11. S. Okur, M. Günes, O. Göktas, F. Finger, and R. Carius. J. Mat. Sci.-Mat. Electron. **15**, 187 (2004). doi:10.1023/B:JMSE.0000011360.00838.c9.
12. S. Okur, O. Göktas, M. Günes, F. Finger, and R. Carius. J. Optoelectron. Adv. Mater. **7**, 491 (2005).
13. R. Brüggemann and N. Souffi. J. Non-Cryst. Solids, **352**, 1079 (2006). doi:10.1016/j.jnoncrysol.2005.11.089.
14. D. Ritter, K. Weiser, and E. Zeldov. J. Appl. Phys. **62**, 4563 (1987). doi:10.1063/1.339051.
15. M. Günes, H. Cansever, G. Yilmaz, M.H. Sagban, V. Smirnov, F. Finger, and R. Brüggemann. Can. J. Phys. **92** (2014). This issue.
16. S. Reynolds, V. Smirnov, F. Finger, C. Main, and R. Carius. Mat. Res. Soc. Symp. Proc. **862**, 525 (2005).
17. S.K. Persheyev, V. Smirnov, K.A. O'Neill, S. Reynolds, and M.J. Rose. Semiconductors, **39**, 343 (2005). doi:10.1134/1.1882798.
18. I. Balberg. Mater. Res. Soc. Symp. Proc. **258**, 693 (1992). doi:10.1557/PROC-258-693.
19. T. Dylla, F. Finger, and R. Carius. Mat. Res. Soc. Symp. Proc. **862**, A.2.5.1 (2003).
20. M. Günes, H. Cansever, G. Yilmaz, V. Smirnov, F. Finger, and R. Brüggemann. J. Non-Cryst. Solids, **358**, 2074 (2012). doi:10.1016/j.jnoncrysol.2012.01.063.